Kinetic model of two-monomer polymerization

Anna C. Nelson, James P. Keener, and Aaron L. Fogelson

Phys. Rev. E **101**, 022501 — Published 4 February 2020

DOI: 10.1103/PhysRevE.101.022501

A kinetic model of two monomer polymerization

Anna C. Nelson*
Department of Mathematics, University of Utah, 155 South 1400 East, Room 233, Salt Lake City, UT 84112-0090, USA

James P. Keener† and Aaron L. Fogelson‡
Departments of Mathematics and Bioengineering, University of Utah, 155 South 1400 East, Room 233, Salt Lake City, UT 84112-0090, USA
(Dated: January 13, 2020)

We propose a kinetic gelation model of polymer growth with two monomeric types that have distinct functionalities (reaction sites), and can polymerize using different reaction types. The heterotypic aggregation of two monomer types is modeled using a moment generating function approach by tracking the temporal evolution of a closed system of moment equations up until gelation. We investigate several scenarios of polymerization with two distinct monomers that differ in the types of reactions that can occur. We determine numerical and analytical conditions for finite time blow-up (the emergence of an oligomer of infinite size) that depend on initial conditions, reaction rates, and number of reaction sites per monomer.

I. INTRODUCTION

General condensation processes have been extensively studied for several decades, and many review papers and books have examined polymerization with gelation [1, 2]. Polymerization models with only a single monomer type have previously been studied using statistical [3, 4], kinetic [5–8], and probabilistic [9, 10] approaches that aim to describe polymerization based on the famous Smoluchowski equation [11]. In the statistical literature, gelation is defined to be the blow-up of the weight-average molecular weight of polymers and is interpreted as a transition of the polymer solution to a gel. It is defined similarly in the kinetic gelation literature and the critical time at which blow-up occurs is called the gel time t_{gel}.

In this paper, we examine the behavior of a system of two types of monomer, type A and type B with three possible reactions: $A-A, A-B$, and $B-B$. We are motivated by our interest in fibrin polymerization during blood clotting. In that process, soluble fibrinogen molecules in the blood plasma are converted into fibrin monomers, which then polymerize to form a gel that is a major structural component of a blood clot [12]. We have previously modeled aspects of fibrin polymerization [13, 14], but in these models, we did not account for the fact that fibrinogen can bind with fibrin but not directly with other fibrinogen molecules. Oligomers of mixtures of fibrinogen and fibrin have been observed experimentally [12, 15–17], and these experiments suggest that this additional type of reaction affects the kinetics of the overall fibrin gelation process. With the ultimate goal of modeling the fibrin-fibrinogen system, here we look at a simplified model, in the belief that our study of it will usefully inform our analysis of the actual biological system.

Others have considered polymerization with mixtures of two monomer types. Goldstein and Perelson [18] considered a two-monomer polymerization system at equilibrium, allowing for binding and unbinding. The authors derived conditions for gelation and discussed how their model applies to experimental results involving basophils and histamine release. A kinetic polymerization system consisting of two distinct monomeric species A and B was introduced by Lushnikov in [19], and subsequent results from this system include oligomer composition distributions and finding exact sol-gel transition times [20, 21].

The Smoluchowski equation for the two monomer condensation system can be written generally as

$$\frac{dc_{m,n}}{dt} = \sum_{k+p=m}\sum_{l+q=n} K(k,l;p,q)c_{k,l}(t)c_{p,q}(t) - \sum_{k,l} K(k,l;m,n)c_{m,n}(t)c_{k,l}(t), \quad (1)$$

where $c_{p,q}$ denotes the concentration of oligomers with p monomers of type A and q monomers of type B. Here, the coagulation kernel $K(k,l;p,q)$ is the reaction rate between a $(k,l)-$mer, containing k monomers of type A and l type B monomers, and an $(p,q)-$mer. In his work, Lushnikov took $K(k,l;m,n)$ to be constant [19] or the product of the masses of the coalescing particles [20, 21]. He also assumed that only heterotypic reactions occur, so reaction sites of the same type do not interact [19].

In the current paper, we assume that reactions between different oligomers occur based on every free binding site having equal probability of reacting with each available binding site on a different oligomer. We also look at situations in which binding sites can participate in multiple types of reactions, both homotypic and heterotypic reactions with rates that can be different for different types of reactions. With these assumptions, our coagulation kernel depends on the types of reactions allowed, and on the number and type of free binding sites avail-

* Corresponding author: anelson@math.utah.edu
† Email: keener@math.utah.edu
‡ Email: fogelson@math.utah.edu

able and so is very different from those considered earlier [11, 18, 19, 22].

In this paper, we present a kinetic gelation model with a kernel that allows for reactions of different types among monomers of types A and B with reaction rates that depend on the concentrations of available reactive sites of each type on the oligomers. The reaction rates are influenced by the functionality (number of reaction sites) of each type of monomer. We vary the composition of the initial mixture of monomers, the monomeric functionality, and the rate constants for the different types of reactions and determine reaction conditions (i.e, combinations of initial composition, functionalities, and reaction rates) that lead to gelation. We explore how the gel time changes, or no longer exists, as the reaction conditions are varied.

Our model is a generalization of the kinetic gelation model presented by Ziff and Stell [5, 6] to study reactions involving a single type of monomer. The Ziff model tracks concentrations c_k of oligomers made up of k identical monomers (k-mers) each with functionality f using an infinite system of ordinary differential equations for c_k, $k = 1, 2, 3, \ldots$. Binding sites on one oligomer can bind with sites on other oligomers to form larger molecules. In this setting, gelation occurs when $\sum_k k^2 c_k \to \infty$, which happens for any nonzero initial concentration of monomer if and only if $f > 2$.

We extend the modeling approach from [5] to a polymerization system that involves oligomers comprised of monomers of two types of monomer, A and B, with f_A reaction sites of type A and f_B reaction sites of type B, respectively. An oligomer C_{ijk} consists of i total monomers with j free reaction sites of type A and k free reaction sites of type B. For example, the monomers of types A and B are denoted $C_{1,f_A,0}$ and $C_{1,0,f_B}$, respectively.

The model allows for three types of reactions: those between A sites on two different oligomers, B sites on two different oligomers, and an A site on one oligomer with a B site on another oligomer. Reaction sites both on the same oligomer are not allowed to react. The rates at which reactions of each type occur depend on the concentrations of free reactive sites of the type involved in that particular reaction. The reactions lead to an infinite set of ordinary differential equations that track the evolution of the concentrations of oligomers of type C_{ijk}, denoted c_{ijk}.

Following [5, 6], we introduce a moment generating function g, derive a partial differential equation for g from the infinite set of ODEs for the concentrations c_{ijk} , and then use g to derive a set of ordinary differential equations for various moments of the oligomer distribution. As we show below, a *closed* system of equations involving the zeroth, first, and second moments is obtained. From these moments we derive expressions for the total concentration of monomers and the average oligomer size, among other interesting physical quantities, and use the small system of ODEs satisfied by the low-moments to study if and when gelation occurs.

II. GENERAL TWO MONOMER POLYMERIZATION

We consider an aggregation system which involves two monomer types: type A monomers, each with f_A reaction sites, and type B monomers, each with f_B reaction sites. Three possible reactions are considered: Binding of a type A site to another type A site, binding of a type A site to a type B site, and binding of a type B site to another type B site. In all cases, the two reacting sites must be on different oligomers, that is, no loops or cycles are allowed to form. The three biomolecular reactions convert two oligomers into a single larger oligomer as shown in Eqs. (2) – (4). As indicated, the respective reactions have (second-order) rate constants k_{AA}, k_{AB}, and k_{BB}.

$$C_{i_1,j_1,k_1} + C_{i_2,j_2,k_2} \xrightarrow{k_{AA}} C_{i_1+i_2,j_1+j_2-2,k_1+k_2}, \tag{2}$$

$$C_{i_1,j_1,k_1} + C_{i_2,j_2,k_2} \xrightarrow{k_{AB}} C_{i_1+i_2,j_1+j_2-1,k_1+k_2-1}, \tag{3}$$

$$C_{i_1,j_1,k_1} + C_{i_2,j_2,k_2} \xrightarrow{k_{BB}} C_{i_1+i_2,j_1+j_2,k_1+k_2-2}. \tag{4}$$

Taking into account the three possible reactions, we assume that the oligomer concentrations $c_{ijk}(t)$ satisfy the following system of ordinary differential equations:

$$\begin{aligned}\frac{dc_{ijk}}{dt} = &\underbrace{\frac{k_{AA}}{2}\left(\sum_{\substack{i_1+i_2=i\\ j_1+j_2=j+2\\ k_1+k_2=k}} j_1 j_2 c_{i_1 j_1 k_1} c_{i_2 j_2 k_2}\right) - k_{AA} j c_{ijk} R_A}_{A\text{-}A \text{ reactions}} \\ &\underbrace{+k_{AB}\left(\sum_{\substack{i_1+i_2=i\\ j_1+j_2=j+1\\ k_1+k_2=k+1}} j_1 k_2 c_{i_1 j_1 k_1} c_{i_2 j_2 k_2}\right) - k_{AB}(k c_{ijk} R_A + j c_{ijk} R_B)}_{A\text{-}B \text{ reactions}} \\ &\underbrace{+\frac{k_{BB}}{2}\left(\sum_{\substack{i_1+i_2=i\\ j_1+j_2=j\\ k_1+k_2=k+2}} k_1 k_2 c_{i_1 j_1 k_1} c_{i_2 j_2 k_2}\right) - k_{BB} k c_{ijk} R_B}_{B\text{-}B \text{ reactions}}.\end{aligned} \tag{5}$$

In this equation, R_A and R_B denote the total concentrations of free type A reaction sites and free type B reaction sites, respectively:

$$R_A = \sum_{i,j,k} j c_{ijk}, \tag{6}$$

	A bind to A	A bind to B	B bind to B
Scenario 1		X	
Scenario 2	X	X	
Scenario 3	X	X	X

TABLE I: Reactions involving monomers of type A and B allowed in each scenario.

and

$$R_B = \sum_{i,j,k} k c_{ijk}. \tag{7}$$

In Eq. (5), the first two terms on the right-hand side describe $A-A$ reactions, the next three terms describe $A-B$ reactions, and the final two terms describe $B-B$ reactions. There are more terms describing $A-B$ reactions because two oligomers can form an $A-B$ bond in two different ways.

There are a number of other quantities of physical interest that we would like to track. These include the total concentration of monomer

$$M = \sum_{i,j,k} i c_{ijk}, \tag{8}$$

and the average number of total monomers in an oligomer or cluster, the average cluster size, defined by

$$\bar{C} = \frac{1}{M} \sum_{i,j,k} i^2 c_{ijk}. \tag{9}$$

To explain why this expression is called the average cluster size, we rewrite it as

$$\bar{C} = \sum_{i,j,k} i\Big(\frac{i c_{ijk}}{M}\Big). \tag{10}$$

Noting that $\sum_{ijk}\left(\frac{i c_{ijk}}{M}\right) = 1$, we see that the expression in parentheses can be interpreted as the probability that a randomly selected monomer will be part of an i-mer, so $\bar{C}$ is the average cluster size. We say that gelation occurs at time t_{gel} if

$$\lim_{t \to t_{gel}^-} \bar{C} \to \infty. \tag{11}$$

We interpret this event as the appearance of an infinite sized cluster.

To aid in the analysis of Eqs. (5), we introduce a generating function similar to Ziff and Stell,

$$g(t,x,y,z) = \sum_{i,j,k} x^i y^j z^k c_{ijk}(t). \tag{12}$$

Using this definition and Eqs. (5), it is straightforward to show that g satisfies the partial differential equation

$$\frac{\partial g}{\partial t} = \frac{k_{AA}}{2}\left(\frac{\partial g}{\partial y}\right)^2 - k_{AA} y \frac{\partial g}{\partial y} R_A + k_{AB}\left(\frac{\partial g}{\partial y}\right)\left(\frac{\partial g}{\partial z}\right) - k_{AB}\left(y\frac{\partial g}{\partial y} R_B + z\frac{\partial g}{\partial z} R_A\right) + \frac{k_{BB}}{2}\left(\frac{\partial g}{\partial z}\right)^2 - k_{BB} z \frac{\partial g}{\partial z} R_B. \tag{13}$$

Using the generating function g, we define moments M_{ijk} by the expressions

$$M_{ijk} = \left.\frac{\partial^{i+j+k} g}{\partial x^i\, \partial y^j\, \partial z^k}\right|_{x=1,y=1,z=1}. \tag{14}$$

In terms of these moments, $R_A = M_{010}$, $R_B = M_{001}$, $M = M_{100}$, and

$$\bar{C} = \frac{M_{200} + M_{100}}{M_{100}}. \tag{15}$$

Using Eqs. (13) and (14), we can derive ordinary differential equations for the low moments. Setting $x = y = z = 1$ in Eq. (13),

$$\frac{dM_{000}}{dt} = -\frac{k_{AA}}{2} R_A^2 - k_{AB} R_A R_B - \frac{k_{BB}}{2} R_B^2. \tag{16}$$

Differentiating all terms in Eq. (13) with respect to y and then setting $x = y = z = 1$ in the result gives the equation

$$\frac{dR_A}{dt} = \frac{dM_{010}}{dt} = -k_{AA} R_A^2 - k_{AB} R_A R_B, \tag{17}$$

while differentiating Eq. (13) with respect to z and setting $x = y = z = 1$ in the result yields

$$\frac{dR_B}{dt} = \frac{dM_{001}}{dt} = -k_{BB} R_B^2 - k_{AB} R_A R_B. \tag{18}$$

Similarly, differentiating Eq. (13) with respect to x and setting $x = y = z = 1$ in the result yields the equation

$$\frac{dM}{dt} = \frac{dM_{100}}{dt} = 0, \tag{19}$$

which ensures conservation of total monomer mass. By computing the appropriate higher partial derivatives of Eq. (13) and setting $x = y = z = 1$, we find differential equations for the second moments

$$\frac{dM_{110}}{dt} = k_{AA}(M_{020} - R_A) M_{110} + k_{AB}\left[M_{110}(M_{011} - R_B) + M_{101} M_{020}\right] + k_{BB} M_{101} M_{011}, \tag{20}$$

$$\frac{dM_{011}}{dt} = k_{AA}(M_{020} - R_A)M_{011} + k_{AB}\left[M_{011}^2 + M_{020}M_{002} - M_{011}(R_A + R_B)\right] + k_{BB}(M_{002} - R_B)M_{011}, \quad (21)$$

$$\frac{dM_{101}}{dt} = k_{AA}M_{110}M_{011} + k_{AB}\left[(M_{011} - R_A)M_{101} + M_{110}M_{002}\right] + k_{BB}(M_{002} - R_B)M_{101}, \quad (22)$$

$$\frac{dM_{200}}{dt} = k_{AA}M_{110}^2 + 2k_{AB}M_{110}M_{101} + k_{BB}M_{101}^2, \quad (23)$$

$$\frac{dM_{020}}{dt} = k_{AA}\left[(M_{020} - 2R_A)M_{020}\right] + 2k_{AB}(M_{011} - R_B)M_{020} + k_{BB}M_{011}^2, \quad (24)$$

$$\frac{dM_{002}}{dt} = k_{AA}M_{011}^2 + 2k_{AB}(M_{011} - R_A)M_{002} + k_{BB}(M_{002} - 2R_B)M_{002}. \quad (25)$$

From the differential equations for the non-negative quantities M_{000}, R_A, and R_B, we see that these quantities are bounded functions of time. Recall that we defined the gelation to occur at time t_{gel} if $\bar{C}(t) \to \infty$ as $t \to t_{gel}^-$. We see that gelation occurs if and only if $M_{200} \to \infty$ at finite time t_{gel}. From Eq. (23) we see that for M_{200} to become unbounded in finite time, at least one of M_{011}, M_{020}, or M_{002} must become unbounded in finite time. Hence, we are interested in determining conditions under which one or more of M_{011}, M_{020}, or M_{002} blow-up in finite time. Note that the equations for R_A, R_B, M_{011}, M_{020}, and M_{002} form a closed system. We study the behavior of this system for the initial conditions $R_A(0) = f_A c_{1f_A0}(0)$, $R_B(0) = f_B c_{10f_B}(0)$, $M_{011}(0) = 0$, $M_{020}(0) = (f_A - 1)R_A(0)$, and $M_{002}(0) = (f_B - 1)R_B(0)$ corresponding to initial concentrations c_{1f_A0} and c_{10f_B} of type A and type B monomers, respectively.

For the remainder of this paper, we consider nondimensionalized versions of Eqs. (17) – (18), (21), (24) – (25). Let $R_T(0) = R_A(0) + R_B(0)$ denote the total initial concentration of free reaction sites. We define the nondimensional time τ as $\tau = t(k_{AB}R_T(0))$, and nondimensional moments $m_{ijk} = M_{ijk}/R_T(0)$. We define nondimensional the $A - A$ and $B - B$ binding rates as $\kappa_{AA} = k_{AA}/k_{AB}$ and $\kappa_{BB} = k_{BB}/k_{AB}$, and a nondimensional initial composition variable

$$\phi = \frac{R_A(0)}{R_T(0)}. \quad (26)$$

The nondimensional ODEs are

$$\frac{dr_A}{d\tau} = -\kappa_{AA}r_A^2 - r_A r_B, \quad (27)$$

$$\frac{dr_B}{d\tau} = -r_A r_B - \kappa_{BB}r_B^2, \quad (28)$$

$$\frac{dm_{011}}{d\tau} = \kappa_{AA}(m_{020} - r_A)m_{011} + m_{011}^2 + m_{020}m_{002} - m_{011}(r_A + r_B) + \kappa_{BB}(m_{002} - r_B)m_{011}, \quad (29)$$

$$\frac{dm_{020}}{d\tau} = \kappa_{AA}(m_{020} - 2r_A)m_{020} + 2(m_{011} - r_B)m_{020} + \kappa_{BB}m_{011}^2, \quad (30)$$

$$\frac{dm_{002}}{d\tau} = \kappa_{AA}m_{011}^2 + 2(m_{011} - r_A)m_{002} + \kappa_{BB}(m_{002} - 2r_B)m_{002}, \quad (31)$$

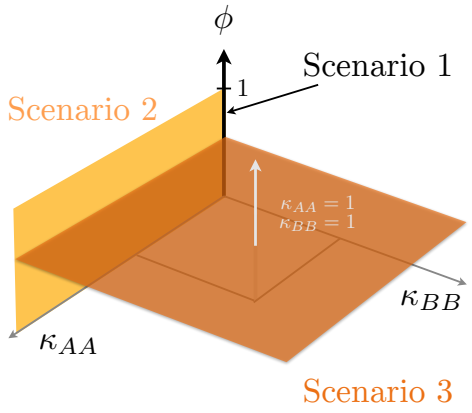

FIG. 1: Schematic of parameter space explored. Scenario 1 corresponds to the vertical ϕ-axis (black) up to 1. Scenario 2 involves exploring the (κ_{AA}, ϕ)-plane (yellow) for $0 \le \phi \le 1$. The orange plane (Scenario 3) explores $(\kappa_{AA}, \kappa_{BB})$ parameter space for $0 \le \phi \le 1$. A special case of Scenario 3 is shown as the grey arrow, when $\kappa_{AA} = \kappa_{BB} = 1$.

with initial conditions

$$m_{020}(0) = (f_A - 1)r_A(0), \quad m_{002}(0) = (f_B - 1)r_B(0), \quad (32)$$

$$r_A(0) = \phi, \quad r_B(0) = 1 - \phi, \quad m_{011}(0) = 0. \quad (33)$$

Throughout the paper, we investigate Eqs. (27) – (31) with different values for the initial conditions and with different reaction rates to determine if and when gelation occurs. Figure 1 illustrates the region of $(\kappa_{AA}, \kappa_{BB}, \phi)$ space that we explore. We first consider the the case in which we set $\kappa_{AA} = 0$ and $\kappa_{BB} = 0$ which we refer to as Scenario 1 corresponding to a portion of the ϕ-axis in Figure 1 (also see Table I). For this case, we derive

analytically inequalities that ϕ must satisfy in order for a gel to form and an analytical formula for the gel time.

We then allow κ_{AA} to be nonzero but keep $\kappa_{BB} = 0$ in Scenario 2, corresponding to the red plane in Figure 1. In this case, we present numerical results on gel occurrence and gel times, using a numerical method described in the next section. Finally, we allow both reaction rates to be nonzero in Scenario 3. We present numerical results for the general case in which $\kappa_{AA} \neq 0$ and $\kappa_{BB} \neq 0$ (the blue plane in Figure 1, and analytical results for the special case $\kappa_{AA} = \kappa_{BB} = 1$ (grey arrow in Fig. 1).

For some conditions, we derive analytic results. For others, we solve the system numerically until finite-time blow-up occurs using a numerical method described in the next section.

III. RESULTS: SCENARIO 1 ($\kappa_{AA} = \kappa_{BB} = 0$)

In a polymerization system with one monomer type with functionality f, gelation is guaranteed to occur in finite time

$$t_{gel}^{ziff} = \frac{1}{kf(f-2)c_1(0)}, \tag{34}$$

where free sites react at rate k and $c_1(0)$ denotes the initial concentration of monomers [5]. For our two monomer polymerization system, we first consider the scenario where the only reaction allowed is the heterotypic binding of A sites to B sites, thus $\kappa_{AA} = \kappa_{BB} = 0$. Under these conditions, Eqs. (27) – (31) reduce to

$$\frac{dr_A}{d\tau} = -r_A r_B, \tag{35}$$

$$\frac{dr_B}{d\tau} = -r_A r_B, \tag{36}$$

$$\frac{dm_{011}}{d\tau} = m_{020}m_{002} - m_{011}(r_A + r_B), \tag{37}$$

$$\frac{dm_{020}}{d\tau} = 2(m_{011} - r_B)m_{020}, \tag{38}$$

$$\frac{dm_{002}}{d\tau} = 2(m_{011} - r_A)m_{002}. \tag{39}$$

We derive conditions on ϕ necessary for gelation to occur in the scenario. Let $w = m_{011} - r_B + \sqrt{m_{020}m_{002}} + \frac{\gamma_0}{2}$, where

$$\gamma_0 = \frac{R_B(0) - R_A(0)}{R_T(0)} = 1 - 2\phi. \tag{40}$$

From the definition of gelation, w will blow-up in finite time if and only at least one of m_{011}, m_{020}, and m_{002} blow-up. Note if m_{011} is bounded then by the form of Eqs. (38) and (39), m_{020} and m_{002} cannot go to zero in finite time. Then

$$\frac{dw}{d\tau} = w^2 - \frac{\gamma_0^2}{4}, \tag{41}$$

and

$$w(0) = \sqrt{(f_A - 1)(f_B - 1)\phi\,(1-\phi)} - \frac{1}{2}. \tag{42}$$

Note that Eq. (41) is separable and

$$w(\tau) = \frac{\gamma_0}{2}\left(\frac{1 + De^{\tau\gamma_0}}{1 - De^{\tau\gamma_0}}\right), \tag{43}$$

where

$$D = \left|\frac{2w(0) - \gamma_0}{2w(0) + \gamma_0}\right|. \tag{44}$$

To find the analytic gel time, we set the denominator of Eq. (43) equal to zero and find

$$\tau_{gel}^{(1)} = \frac{\ln\left(2w(0) + \gamma_0\right) - \ln\left(2w(0) - \gamma_0\right)}{\gamma_0}. \tag{45}$$

Note that $\tau_{gel}^{(1)}$ is defined only if both $2w(0) + \gamma_0 > 0$ and $2w(0) - \gamma_0 > 0$, which implies

$$\frac{1}{(f_A - 1)(f_B - 1) + 1} < \phi < \frac{(f_A - 1)(f_B - 1)}{(f_A - 1)(f_B - 1) + 1}. \tag{46}$$

The bounds in Eq. (46) require either $f_A > 2$ or $f_B > 2$, which is the same requirement needed for the system to gel in [5]. In order to gel in finite time, it must also be true that $f_A > 1, f_B > 1$. If a monomer has functionality less than 2, one can intuitively consider that monomer to be an 'inhibitor' of the system, where it binds to an available free site and removes it from the system. However, if both monomers have functionality greater than 2 there still exists an upper and lower in ϕ for gelation to occur. Since type A monomers can bind only to type B monomers, the gelation properties of the polymerization system depend not only on the functionalities but also on the relative initial concentrations of free reaction sites of the two types. Figure 2a shows how the gel time given in Eq. (45) varies with ϕ, the fraction of initial reaction sites that are type A, for various combinations of functionalities.

Reflecting the bounds in Eq. (46), we see that there are combinations of functionalities and initial conditions for which gelation (i.e., finite-time blow up of $\bar{C}$) does not occur in the case in which only heterogeneous $A-B$ binding occurs. For each pair of functionalities, gelation does not occur if there is excess of either monomer types. For example, if $f_A = 3$ and $f_B = 2$, gelation happens only for $1/3 < \phi < 2/3$. If either reaction site type initially comprises more than $2/3$ of the total initial reaction sites,

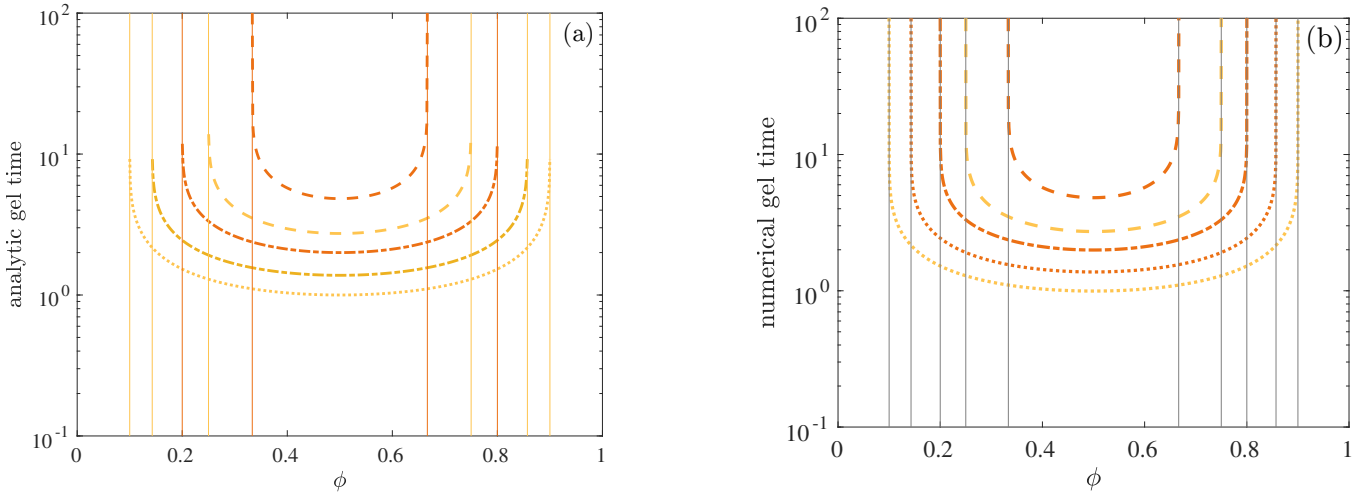

FIG. 2: Scenario 1 ($\kappa_{AA} = \kappa_{BB} = 0$): (a) Analytical gel time $\tau_{gel}^{(1)}$ and (b) numerical gel time τ_{gel}^{num} gel time as functions of ϕ and for various functionality combinations: $f_A = 3$ (orange), $f_A = 4$ (yellow), $f_B = 2$ (dashed), $f_B = 3$ (dot-dashed), $f_B = 4$ (dotted). Vertical lines correspond to lower and upper bounds found in Eq. (46).

gelation does not occur. For larger functionalities, the interval of ϕ values for which gelation occurs becomes larger, as expected, but for each functionality pair, the interval has a left-end greater than 0 and a right-end less than 1. In addition, for a given value of ϕ, $\tau_{gel}^{(1)}$ decreases implying that gelation occurs earlier.

For the other scenarios listed in Table I, we are unable to find analytic bounds on ϕ that ensure gelation nor an analytic formula for the gel time, and so we evaluate the time evolution of the moment system Eqs. (27) – (31) numerically. We define 'numerical blow up' to occur if the sum of the moments m_{020}, m_{002}, and m_{011} becomes larger than 10^7, and we define the 'numerical gel time' to be the time at which this occurs, denoted as τ_{gel}^{num}. The moment equations are solved up to $\tau_{end} = 10^6$ if numerical blow up does not occur, and in that case we set $\tau_{gel} = \tau_{end}$. Figure 2b shows the results of using this numerical approach to determining gelation properties in Scenario 1. Comparing the results with the analytic ones in Figure 2a, we see excellent agreement, thus validating the use of this numerical approach in Scenarios 2 and 3.

IV. RESULTS: SCENARIO 2 ($\kappa_{BB} = 0$)

In this section we set $\kappa_{AA} > 0$ while keeping $\kappa_{BB} = 0$ in order to explore the behavior of the moment equations in the case that $A - A$ binding is allowed in addition to the $A - B$ binding considered in Scenario 1. Typical oligomers for various parameter ranges are shown in Fig. 3.

Since introducing the additional type of binding changes the structure of the moment equations, the gel time given in Eq. (45) is no longer applicable. Instead, we present numerical results obtained with the numerical finite-time blow up approach described at the end of Section III. The nondimensional moment equations for Scenario 2 are Eqs. (27) – (31) with $\kappa_{BB} = 0$:

$$\frac{dr_A}{d\tau} = -\kappa_{AA} r_A^2 - r_A r_B, \tag{47}$$

$$\frac{dr_B}{d\tau} = -r_A r_B, \tag{48}$$

$$\frac{dm_{011}}{d\tau} = \kappa_{AA}(m_{020} - r_A)m_{011} + m_{011}^2 + m_{020}m_{002} - m_{011}(r_A + r_B), \tag{49}$$

$$\frac{dm_{020}}{d\tau} = \kappa_{AA}\left[(m_{020} - 2r_A)m_{020}\right] + 2(m_{011} - r_B)m_{020}, \tag{50}$$

$$\frac{dm_{002}}{d\tau} = \kappa_{AA} m_{011}^2 + 2(m_{011} - r_A)m_{002}. \tag{51}$$

Figure 4 shows how the numerical gel time varies with ϕ for various pairs of functionalities when $\kappa_{AA} = 1$ and $\kappa_{BB} = 0$. As before, line colors black, blue, and red correspond to $f_A = 2$, $f_A = 3$, and $f_A = 4$, respectively, and the dashed, dot-dashed, and dotted line styles represent $f_B = 2$, $f_B = 3$, and $f_{BB} = 4$, respectively. For the cases in which $f_A > 2$, as $\phi \to 1$, the computed gel time approaches that found in [5] for gelation with a single type of monomer. When $\phi = 1$, there is only type A monomer in our system. For $f_A = 2$, the numerical gel time approaches infinity, indicating that no gel forms, consistent

with the necessary condition that monomer functionality be larger than 2 in the single monomer type situation [5]. For each of the functionality pairs depicted in Figure 4, there is a lower bound such that when ϕ is lower than this bound, gelation does not occur. The lower bounds are close to but not the same as those found in Scenario 1, e.g., for $f_A = 3$ and $f_B = 2$, the approximate lower bound here is $\phi = 0.3193$, while that in Scenario 1 is $\phi = \frac{1}{3}$.

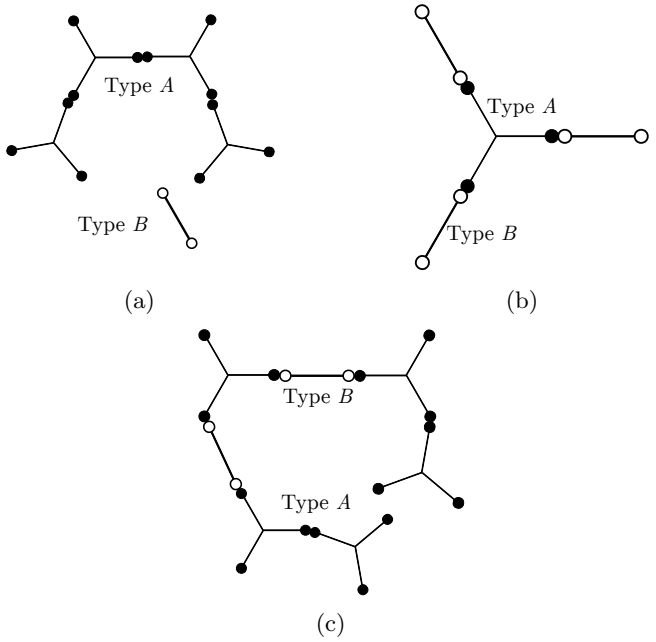

FIG. 3: Typical oligomers for various parameter combinations for Scenario 2, with $f_A = 3, f_B = 2$. (a) $\kappa_{AA} >> 1$, $\phi \approx 1$. (b) $\kappa_{AA} << 1$, $\phi << 1$. (c) $\kappa_{AA} \approx 1$, ϕ intermediate.

Figure 5 illustrates how numerical gel time changes with the reaction rate κ_{AA} and the initial available binding composition ϕ. In order to demonstrate what would occur if a monomer that can gel on its own was added to a system that cannot gel, we let $f_A = 3$ and $f_B = 2$. This choice is also motivated by the polymerization of fibrin and fibrin-fibrinogen interactions. The white region in Fig. 5 corresponds to parameter values that have no finite time blow-up and the colored area corresponds to parameter values that lead to the formation of a gel. Note that when $\kappa_{AA} = 0$ (corresponding to the x-axis), a lower and upper bound for gelation in ϕ exists, given in Eq. (46). The upper bound in ϕ exists only for $\kappa_{AA} = 0$. Assuming $f_A > 2$, type A monomers can bind to other type A monomers for even small κ_{AA}, which eventually lead to the formation of a gel. A relative deficiency in type B reaction sites ($\phi \approx 1$) does not inhibit gelation in this case.

We compare the theoretical gel time from Ziff [5] with the numerical gel time for Scenario 2 to determine if adding an additional monomer and reaction type hinders

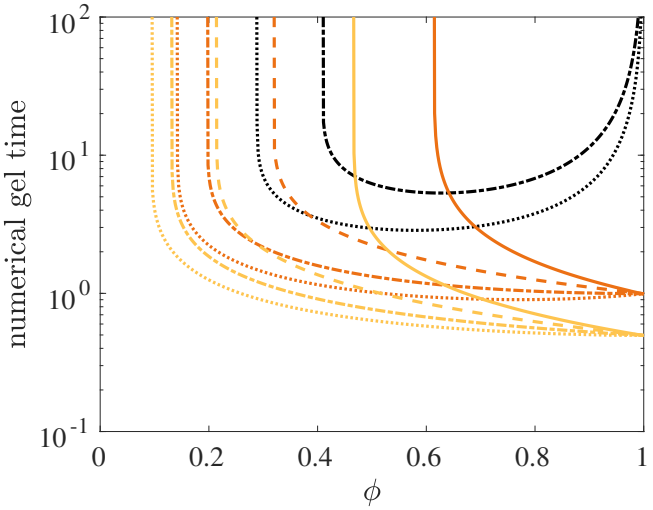

FIG. 4: Scenario 2 ($\kappa_{BB} = 0$): Numerical gel time as a function of ϕ for $\kappa_{AA} = 1$ and various functionality combinations: $f_A = 2$ (black), $f_A = 3$ (orange), $f_A = 4$ (yellow), $f_B = 1$ (solid), $f_B = 2$ (dashed), $f_B = 3$ (dot-dashed), $f_B = 4$ (dotted).

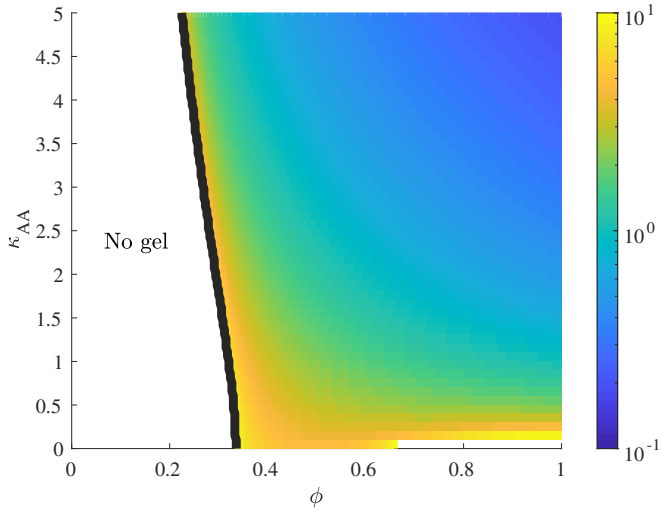

FIG. 5: Scenario 2 ($\kappa_{BB} = 0$): Numerical gel time as a function of ϕ and κ_{AA}. The functionalities are fixed ($f_A = 3, f_B = 2$). The color bar indicates when finite time blow-up occurred.

or helps gelation. Let τ_{gel}^{ziff} be the theoretical Ziff gel time. Figure 6 shows τ_{gel}^{num} curves (solid curves) for various κ_{AA} values, corresponding to horizontal slices of Fig. 5, and τ_{gel}^{ziff} gel times (dashed curves) with one monomer, functionality $f = 3$, polymerizing [5]. For large κ_{AA} (orange), τ_{gel}^{num} is monotonically decreasing in ϕ while for small κ_{AA} (yellow), τ_{gel}^{num} is non-monotonic in ϕ. For $\phi = 1$, $\tau_{gel}^{num} = \tau_{gel}^{ziff}$.

Numerical gel times for large κ_{AA} are longer than the theoretical Ziff gel time for $\phi < 1$, indicating that for

large κ_{AA}, adding an additional monomer and reaction causes the system to more slowly. In Fig. 6, for each κ_{AA} value, there is a lower bound for ϕ, below which the numerical gel time, τ_{gel}^{num}, indicates that no gelation has occurred. For κ_{AA} small (red) then for large and intermediate values of ϕ, $\tau_{gel}^{num} < \tau_{gel}^{ziff}$ implying that the $A-B$ reactions speed up gelation. For low ϕ values, $\tau_{gel}^{num} > \tau_{gel}^{ziff}$ implying that the $A-B$ reactions hinder gelation, or prevent it all together. Hence, compared to gelation in a pure type A system, the presence of type B monomers and $A-B$ reactions can either hinder or accelerate gelation when κ_{AA} is small.

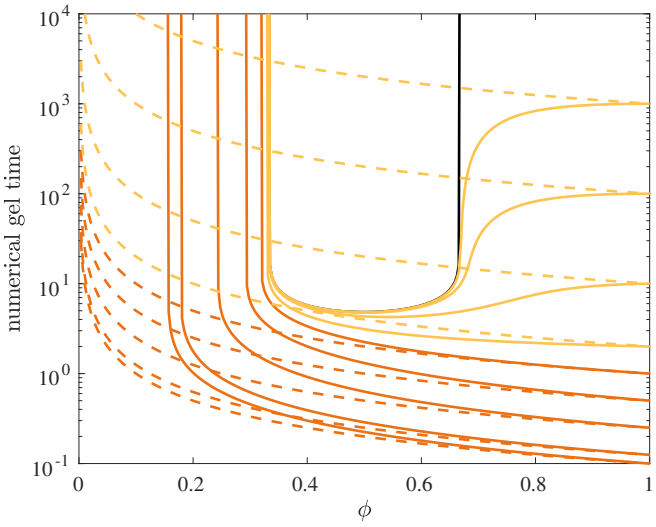

FIG. 6: Scenario 2 ($\kappa_{BB} = 0$): τ_{gel}^{num} (solid curves) as a function of ϕ with varying κ_{AA} ($f_A = 3, f_B = 2$) with τ_{gel}^{ziff}, for $f = 3$ functionality [5]. Yellow curves indicate $\kappa_{AA} < 1$ and orange curves indicate $\kappa_{AA} \geq 1$. From bottom to top, solid curves are for $\kappa_{AA} = 10$, 8, 4, 2, 1, 0.5, 0.1, 0.01, 0.001, and 0.

In Figure 5, there is a clear boundary, or separatrix, indicated in black, separating values of (ϕ, κ_{AA}) for which a gel forms or for which a gel does not form. We show in Figure 7 how the location of the boundary curve changes as the functionalities of f_A and f_B are altered. For the (f_A, f_B) combination for which gelation would occur in a pure type A system ($f_A \geq 3$), the minimum level of ϕ needed for gelation decreases as κ_{AA} increases, i.e. gelation occurs for a wider range of initial compositions. For $f_A = 2, f_B = 3$, the lower bound on ϕ increases as κ_{AA} increases, so gelation occurs for a narrower range of initial compositions. We also see that fixing one functionality (f_A or f_B), the range of compositions allowing gelation increases as the other functionality is increased.

V. RESULTS: SCENARIO 3 (ALL REACTIONS ALLOWED)

The final scenario discussed is that in which κ_{AA} and κ_{BB} are both nonzero so type $A-A$, type $A-B$, and type $B-B$ reactions can all occur. We investigate two cases, the first in which $\kappa_{AA} = \kappa_{BB} = 1$ so all reaction rates are equal, or the general case where κ_{AA} and κ_{BB} can be any nonnegative value. Thus, we investigate the original nondimensional moment equations Eqs. (27) – (31).

A. Reaction rates equal ($\kappa_{AA} = \kappa_{BB} = 1$)

We assume that the three types of reactions occur at the same rate; thus, $\kappa_{AA} = \kappa_{BB} = 1$ in Eqs. (27) – (31). Since the reaction rates are all equal, the reactivities of monomer types A and B depend only on their functionalities, f_A and f_B, respectively. Letting $v(t) = m_{020} + m_{002} + 2m_{011} - r_A - r_B$, it follows from Eqs. (27) – (31), that

$$\frac{dv}{d\tau} = v^2. \tag{52}$$

Solving this equation yields

$$v(\tau) = \frac{v(0)}{1 - v(0)\tau}. \tag{53}$$

where $v(0) = (f_A-2)r_A(0)+(f_B-2)r_B(0)$. A gel appears if $v \to \infty$, which occurs at time

$$\tau_{gel}^{(3)} = \frac{1}{(f_A-2)r_A(0) + (f_B-2)r_B(0)}, \tag{54}$$

provided this quantity is positive. If $f_A = f_B = f$, then $r_A(0) = r_B(0) = f\tilde{c}(0)$ where $\tilde{c}(0) = c_{1,f_A,0}+c_{1,f_B,0}$ is the total initial concentrations of the two types of monomers in the system. Using these in Eq. (54), we obtain

$$\tau_{gel}^{ziff} = \frac{1}{f(f-2)\tilde{c}(0)}, \tag{55}$$

which is the gelation time from the Ziff-Stell model [5]. Note in particular that if $f_A = f_B = 2$, a gel does not form. We next investigate the effect of varying f_A and f_B on $\tau_{gel}^{(3)}$ given in Eq. (54). We again let $\phi = r_A(0)$, and write the expression in Eq. (54) as

$$\tau_{gel}^{(3)} = \frac{1}{f_B - 2 + (f_A - f_B)\phi}. \tag{56}$$

Figure 8 shows how $\tau_{gel}^{(3)}$ varies with ϕ for several f_A, f_B combinations. For each pair of f_A, f_B values, with $f_A > f_B$, $\tau_{gel}^{(3)}$ decreases as ϕ increases to 1, while $\tau_{gel}^{(3)}$ increases as ϕ increases to 1 if $f_A < f_B$. No gel forms

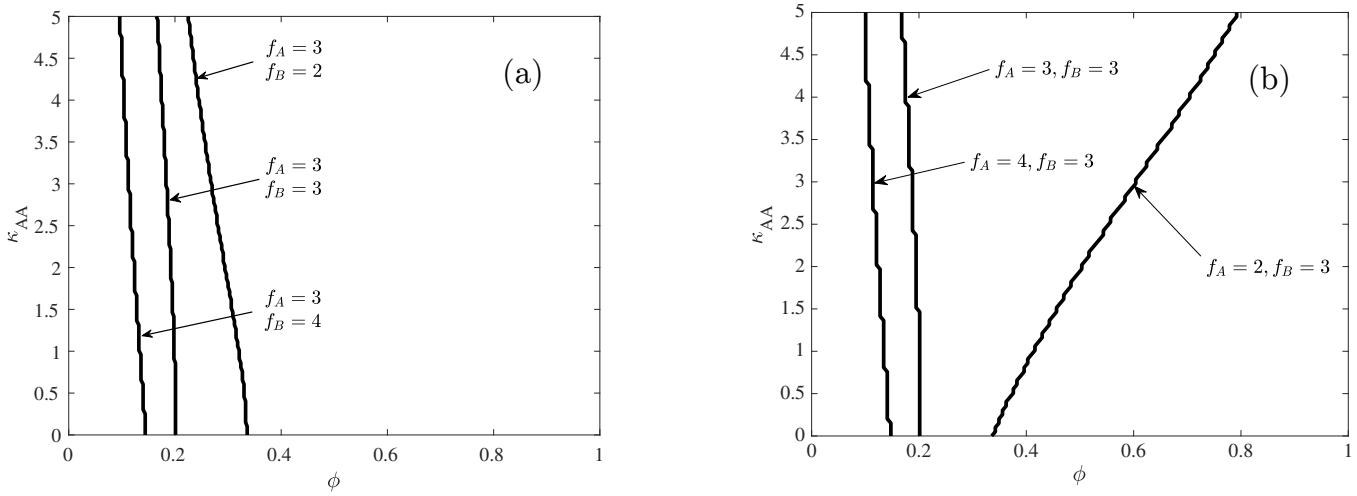

FIG. 7: Scenario 2 ($\kappa_{BB} = 0$): Gel-no gel boundaries similar to Fig. 5 for fixed f_A (a) and f_B (b) functionality. To the left of each curve, gelation does not occur and to the right of the curve, gelation occurs for given (ϕ, κ_{AA}).

for $f_A = f_B = 2$ (not shown) or for $\phi = 0$ and $f_B = 2$. When $f_B = 1$, Eq. (56) becomes

$$\tau_{gel}^{(3)} = \frac{1}{(f_A - 1)\phi - 1}. \tag{57}$$

Since $\tau_{gel}^{(3)} < 0$ is impossible, we must have that

$$\phi > \frac{1}{f_A - 1} \tag{58}$$

for gelation to occur in this case.

From Fig. 8 we see that $\tau_{gel}^{(3)}$ depends on both monomer functionalities. If $f_A \neq f_B$, then an increase in either value results in faster gelation. For example, with $f_A = 3$, $f_B = 2$, and $\phi = 0.5$, $\tau_{gel}^{(3)} \approx 2$, but for the same ϕ value and $f_A = 4$, $f_B = 2$, $\tau_{gel}^{(3)} \approx 1$. The solid curves in Fig. 8 ($f_B = 1$) reflect the gel times when the inequality in Eq. (58) (vertical) must hold. From Equation (55), if $f_A = 2$ or $f_B = 2$ and the other functionality is greater than 2, $\tau_{gel}^{(3)}$ does not depend on monomer A or monomer B, respectively, and $\tau_{gel}^{(3)} = \tau_{gel}^{ziff}$. The situation corresponds to the dashed curves and the black curves in Fig. 8. If $f_A = f_B$ then type A and type B monomers are indistinguishable since all reaction rates are equal, thus the gel time does not depend on ϕ (flat curves in Fig. 8). This particular gel time is equivalent to that from Eq. (55) for $\tilde{c}(0) = 1$.

It is clear that the gel time depends on the initial composition variable ϕ. Figure 8 illustrates that for any functionality combination in which $f_A > 2$, as ϕ increases to 1, $\tau_{gel}^{(3)}$ approaches the gel time τ_{gel}^{ziff} from Eq. (55) for the single monomer system with functionality f_A and initial concentration $\tilde{c}(0) = 1$ [5]. For functionality combinations in which gelation can occur for $0 \leq \phi \leq 1$, gel time curves begin at the τ_{gel}^{ziff} for functionality f_B and end at τ_{gel}^{ziff} time for f_A. For example, when $f_A = 4, f_B = 3$ (yellow, dot-dashed curve), at $\phi = 0$ the gel time corresponds to τ_{gel}^{ziff} with functionality $f_B = 3$ and at $\phi = 1$ the gel time is equal to τ_{gel}^{ziff} with functionality $f_A = 4$.

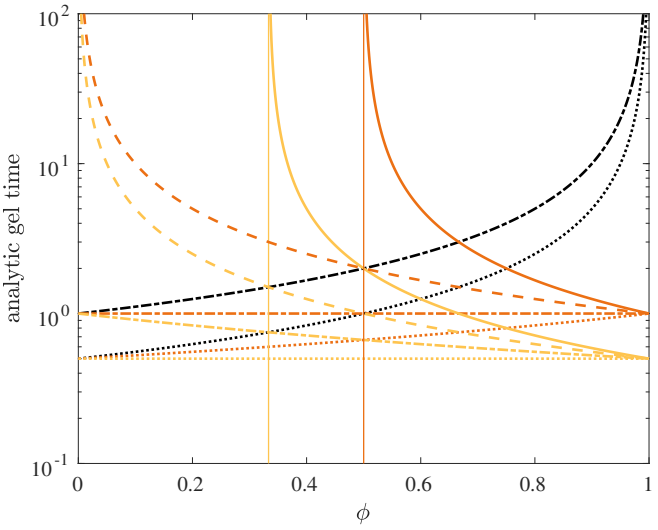

FIG. 8: Analytical gel time $\tau_{gel}^{(3)}$ as a function of ϕ with various functionality combinations: $f_A = 2$ (black), $f_A = 3$ (orange), $f_A = 4$ (yellow), $f_B = 1$ (solid), $f_B = 2$ (dashed), $f_B = 3$ (dot-dashed), $f_B = 4$ (dotted). Flat curves ($f_A = f_B$) are equivalent to τ_{gel}^{ziff}.

B. General case

We next investigate Scenario 3 with reaction rates κ_{AA} and κ_{BB} set to arbitrary positive values. No analytic formula for the gel time is available, so we solve Eqs. (27) – (31) numerically until finite-time blow up occurs using the method described for Scenario 1. With all reaction rates positive, a gel forms in finite time if $f_A > 2$ or $f_B > 2$. Figure 9 shows $\tau_{gel}^{(3)}$ as a function of κ_{AA} and κ_{BB} for $f_A = 4$, $f_B = 3$, and $\phi = 0.2$. Note that the maximum gel time is order 10, indicating that a gel always forms quickly (relative to gel times found in Scenarios 1 and 2) and the slowest gel formation occurs when both κ_{AA} and κ_{BB} are small. For $\tau_{gel}^{(3)}$ plots

Figure 10 shows how the gel time depends on ϕ with $\kappa_{AA} = 10^{-1}$ and $\kappa_{BB} = 10^{-4}$. The figure also shows τ_{gel}^{ziff} for functionality $f = 3$ and rate constant $k = 10^{-4}$ and for functionality $f = 4$ and rate constant $k = 10^{-1}$, as well as the gel time $\tau_{gel}^{(1)}$ from Scenario 1 (when $\kappa_{AA} = \kappa_{BB} = 0$). Note that a gel forms for both $\phi = 0$ and $\phi = 1$, and that τ_{gel}^{num} equals the τ_{gel}^{ziff} value. In these cases $f = 3, k = 10^{-4}$ and $f = 4, k = 10^{-1}$, respectively.

The sizes of κ_{AA} and κ_{BB} influence how close the numerical gel time for Scenario 3B is to the analytical gel time for Scenario 1. Since κ_{AA} is far from zero, the blue curve does not hug the dashed curve in Fig. 10. With $\kappa_{BB} = 10^{-4}$, the numerical gel time for Scenario 3 agrees with the Scenario 1 gel time for intermediate ϕ. Since there are more free B sites and κ_{BB} is relatively closer to zero, we see good agreement for $\frac{1}{3} < \phi < \frac{1}{2}$. As ϕ increases, this agreement no longer holds as there are more A sites available and κ_{AA} is far from zero.

We next look at the specific case $f_A = 3$ and $f_B = 2$, in which monomer B on its own cannot form a gel, and determine the conditions under which a gel can form in the two monomer system. Figure 11 shows τ_{gel}^{num} as a function of κ_{AA} and κ_{BB} for $\phi = 0.2$. Point (a) shows the (approximate) parameter values for Scenario 1, and point (c) shows the parameter values for Scenario 3A, and point (b) shows the parameter values for Scenario 2 with $\kappa_{AA} = 1$. To understand how τ_{gel}^{num} changes as parameter value variations move the system between the different scenarios listed in Table 1, we perform sets of simulations using parameter values from points along the numbered paths in Figure 10. For each parameter point, the gel time τ_{gel}^{num} is computed as a function of the initial composition variable ϕ.

Gel time vs. ϕ curves from points along the transition paths 1 to 6 are shown in Figure 12. Figure 12a illustrates the transition between Scenarios 1 and 2 along path 1 where $\kappa_{BB} = 0$ and κ_{AA} increases from 0 to 1, and between Scenarios 2 and 3 along path 2 where $\kappa_{AA} = 1$ and κ_{BB} increases from 0 to 1. The solid black curve shows $\tau_{gel}^{num}(\phi)$ for Scenario 1 in which $\kappa_{BB} = 0$ and $\kappa_{AA} = 0$ showing that gelation occurs only for $1/3 < \phi < 2/3$ in

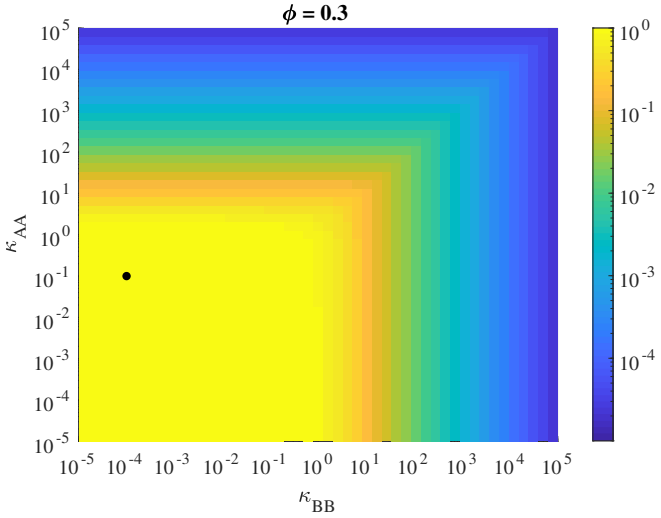

FIG. 9: Scenario 3 ($\kappa_{AA} \neq \kappa_{BB}$): Numerical gel time for $f_A = 4, f_B = 3$. Heatmap of gel times as a function of κ_{AA}, κ_{BB} for $\phi = 0.3$, $\tau_{end} = 10^6$. Black data point corresponds to parameter values found in Figure 10.

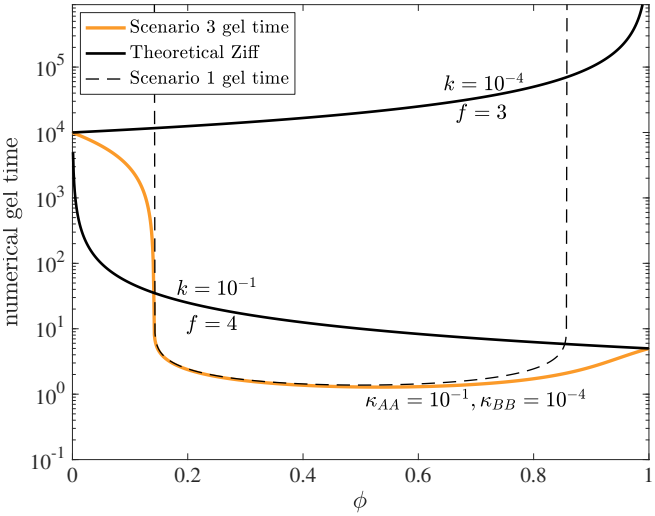

FIG. 10: Scenario 3 ($\kappa_{AA} \neq \kappa_{BB}$): Numerical gel time as a function of ϕ for $\kappa_{AA} = 10^{-1}, \kappa_{BB} = 10^{-4}$ for $f_A = 4, f_B = 3$. Vertical lines indicate gelation bounds from Scenario 1. Black curves indicate theoretical Ziff times for $f = 4$ and $f = 3$.

this case. As κ_{AA} increases from 0 to 1 along path 1, the dashed red curves show how gel time decreases substantially for $\phi > 2/3$, moderately for $1/3 < \phi < 2/3$, and how the lower bound on gel formation moves increasing but always small steps to the left. The limiting solid red curve for $\kappa_{AA} = 1$ and $\kappa_{BB} = 0$ for Scenario 2 shows that the lower bound from Scenario 1 persists at a slightly smaller value for Scenario 2. The dashed blue curves show how the gel time decreases for $\phi < 1/3$ for parameter values along path 2 as the system moves

between Scenario 2 and Scenario 3A.

Similar curves are shown in Figures 12b. Again, the solid black curve refers to $\tau_{gel}^{num}(\phi)$ for Scenario 1. The dashed red curves indicate how the gel time changes as κ_{AA} increases from 0 to 1 along path 3. The upper bound for gelation moves to the left, while the lower bound decreases considerably for $\phi < 1/3$ and moderately for $1/3 < \phi < 2/3$. The solid red curve for $\kappa_{BB} = 1, \kappa_{AA} = 0$ illustrates that the upper bound persists, although for a smaller value of ϕ than in Scenario 1. Gel times along path 4 are indicated by dashed blue lines, where gel times decrease for $\phi > 2/3$, and as κ_{BB} approaches 1, we obtain the gel time found in Scenario 3A (solid blue).

Figure 12c shows how gel times change along paths 4 and 5. The dashed red curves reveal how gel time changes as we set $\kappa_{AA} = 0$ and vary $1 < \kappa_{BB} < 10^5$. Note that in the limit when $\kappa_{BB} >> 1$, no gelation can occur since the functionality of monomer B is two. As κ_{BB} decreases from 10^5, the upper ϕ bound for gelation increases substantially to the same red curve found in Fig. 12b. Path 4 curves shown in Fig. 12c are identical to those in Fig. 12b and show how gel times approach Scenario 3A as we increase κ_{AA} to 1.

Path 6 illustrates how the gel times transition from $\kappa_{AA} = 0, \kappa_{BB} = 10^5$ (solid black) to $\kappa_{AA} = 1, \kappa_{BB} = 10^5$. As κ_{AA} is varied and increases towards 1, the system gels more quickly (dashed grey). When $\kappa_{AA} = 1, \kappa_{BB} = 10^5$, the dashed grey curve lies on top of the τ_{gel}^{ziff} curve. Since $f_B = 2$, increasing $\kappa_{BB} > 1$ does not change the gel time of the system.

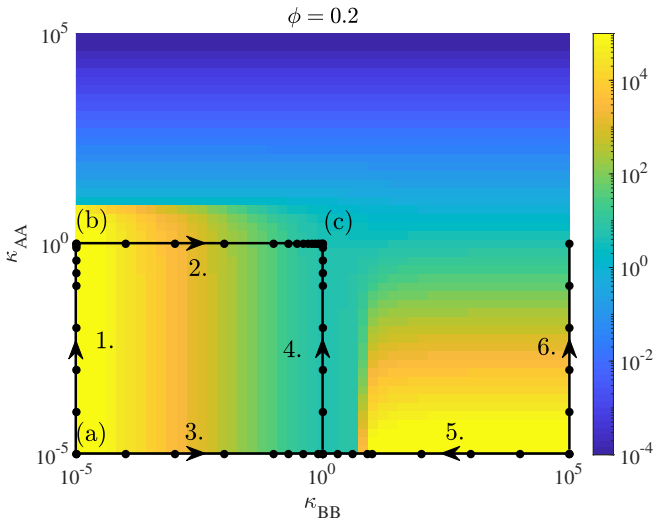

FIG. 11: Gel times for polymerization system with $f_A = 3, f_B = 2$, varying reaction rates, and $\phi = 0.2$. (a), (b), (c) on plot marks Scenario 1, Scenario 2, and theoretical Ziff times for $\phi = 0.2$, respectively. Transitions from scenarios are marked 1. through 6.

VI. DISCUSSION

We have presented a two-monomer polymerization system with a coagulation kernel based on the number of available binding sites and on the types of reactions each binding site can participate in. We assumed no intramolecular reactions thus no cycles can form on oligomers. Several authors have proposed polymerization systems with intramolecular reactions involving one [7, 23, 24] or two [25] monomer species, and find that cycle formation affect the sol-gel transition time.

Without allowing cycles, the reactions we allow the system to participate in are incorporated into a kinetic gelation model that is comprised of an infinite set of concentrations c_{ijk}, one for each oligomer with a specific total number of oligomers, free reaction sites of type A and free reaction sites of type B. Using an approach similar to that of Ziff and Stell in [5], we found a closed system of low order moment equations that can be analyzed up until gelation with varying possible reaction rates, monomer functionalities, and initial concentration of available reaction sites.

When all reaction rates are equal, we derived an analytical gelation time that was numerically validated by solving the closed system until finite-time blow-up occurs. The analytical gel time depended on the functionality of each monomer type and on the initial concentration of free binding sites available. A gel formed in all cases except when at least one of the monomer functionalities is equal to 1. If a given monomer has only one binding site, it binds to a free binding site and occupies it, thus removing a free site from the system. If initially there is monomer with $f_B = 1$ in excess, no gel forms. Therefore, there exists a lower bound on ϕ, the ratio of initial concentration of free type A binding sites to the total initial binding site concentration, for finite-time blow-up for only one functionality value $f_B = 1$.

We numerically investigated the polymerization system where no $B - B$ reactions occur. For each f_A, f_B combination, gelation does not occur for small ϕ values so a minimum ϕ exists for gelation to occur. As f_A and f_B increases, this threshold in ϕ decreases so less A monomers are required to gel.

For a system in which only heterogeneous reactions can occur ($k_{AA} = k_{BB} = 0$), if there are too few reaction sites of type A, gelation cannot occur since B cannot react with B. Similarly, if there are too many reactions sites of type A, gelation cannot occur. An analytical gel time was obtained for this scenario, and upper and lower bound sin ϕ on gelation was found and confirmed using numerical simulations. The case allowing only heterogeneous reactions has been investigated previously using a probabilistic approach based on branching processes [9, 10], where the authors obtain similar results for the case $f_B = 2$.

Based on the results presented, it is clear that gelation depends not only on the amount of monomer initially present, but also on the functionality of each monomer

in the polymerization system. In the multicomponent gelation literature, previous work has studied systems that react according to the mass of monomers present in oligomer, and does not include the functionality of monomers. Gelation is not possible if both monomers have only two free reaction sites, so it is critical to incorporate monomeric functionality into any mathematical model.

[1] D. J. Aldous. Deterministic and Stochastic Models for Coalescence (Aggregation and Coagulation): A Review of the Mean-Field Theory for Probabilists. *Bernoulli*, 5(1):3, 1999. ISSN 13507265. doi:10.2307/3318611. URL `http://www.jstor.org/stable/3318611?origin=crossref`.

[2] E. Ben-Naim P.L. Krapivsky, Redner S. *A Kinetic View of Statistical Physics*. Cambridge University Press, Cambridge, 2010.

[3] P. J. Flory. Molecular size distribution in three dimensional polymers. *Journal of the American Chemical Society*, 63(11):3083–3090, 1941. doi:10.1021/ja01856a061. URL `https://doi.org/10.1021/ja01856a061`.

[4] W. H. Stockmayer. Theory of molecular size distribution and gel formation in branched-chain polymers. *The Journal of Chemical Physics*, 11(2):45–55, 1943. ISSN 00219606. doi:10.1063/1.1723803.

[5] R.M. Ziff and G. Stell. Kinetics of polymer gelation. *Journal of Chemical Physics*, 73(3492), 1980. doi: https://doi.org/10.1063/1.440502.

[6] R.M. Ziff. Kinetics of polymerization. *Journal of Statistical Physics*, 22(2):241–263, 1980. doi: https://doi.org/10.1007/BF01012594.

[7] R. M. Ziff, E. M. Hendricks, and M. H. Ernst. Critical Properties for Gelation: A Kinetic Approach. *Physical Review Letters*, 49(8):593–595, 1982. doi: https://doi.org/10.1103/PhysRevLett.49.593.

[8] A. A. Lushnikov. Exactly solvable model of a coalescing random graph. *Physical Review E - Statistical, Nonlinear, and Soft Matter Physics*, 91(022119), 2015. doi: 10.1103/PhysRevE.91.022119.

[9] D. R. Miller and C. W. Macosko. A New Derivation of Post Gel Properties of Network Polymers. *Macromolecules*, 9(2):206–211, 1976. doi: 10.1021/ma60050a004.

[10] C. W. Macosko and D. R. Miller. A New Derivation of Average Molecular Weights of Nonlinear Polymers. *Macromolecules*, 9(2):199–206, 1976. doi: 10.1021/ma60050a003.

[11] M. V. Smoluchowski. Versuch einer mathematischen theorie der koagulationskinetik kolloider lösungen. *Z. Phys. Chem.*, 92:129 – 168, 1917.

[12] J. W. Weisel. Fibrinogen and fibrin. *Advances in Protein Chemistry*, 70, 2005. doi:10.1016/S0065-3233(05)70008-5.

[13] R. D. Guy, A. L. Fogelson, and J. P. Keener. Fibrin gel formation in a shear flow. *Mathematical Medicine and Biology: A Journal of the IMA*, 24(1):111–130, 2007. doi: 10.1093/imammb/dql022. URL `+http://dx.doi.org/10.1093/imammb/dql022`.

[14] A. L. Fogelson and J. P. Keener. Toward an understanding of fibrin branching structure. *Phys. Rev. E*, 81:051922, May 2010. doi:10.1103/PhysRevE.81.051922. URL `https://link.aps.org/doi/10.1103/PhysRevE.81.051922`.

[15] L. A. Chtcheglova, A. Haeberli, and G. Dietler. Force spectroscopy of the fibrin(ogen)–fibrin interaction. *Biopolymers*, 89(4):292–301, 2007. doi: 10.1002/bip.20910.

[16] M. Rocco, S. Bernocco, M. Turci, A. Profumo, C. Cuniberti, and F. Ferri. Early events in the polymerization of fibrin. *Annals of the New York Academy of Sciences*, 936(1):167–184, 2001. doi:10.1111/j.1749-6632.2001.tb03504.x. URL `https://nyaspubs.onlinelibrary.wiley.com/doi/abs/10.1111/j.1749-6632.2001.tb03504.x`.

[17] A. Henschen. On the identity of fibrin(ogen) oligomers appearing during fibrin polymerization. In *Fibrinogen, Thrombosis, Coagulation, and Fibrinolysis*, volume 281, pages 49–53. Springer, 1990. doi: https://doi.org/10.1007/978-1-4615-3806-6˙4.

[18] B. Goldstein and A. S. Perelson. Equilibrium theory for the clustering of bivalent cell surface receptors by trivalent ligands. Application to histamine release from basophils. *Biophysical Journal*, 45(6):1109–1123, 1984. ISSN 0006-3495. doi:10.1016/S0006-3495(84)84259-9. URL `http://dx.doi.org/10.1016/S0006-3495(84)84259-9`.

[19] A. A. Lushnikov. Evolution of coagulating systems: III. Coagulating mixtures. *Journal of Colloid And Interface Science*, 54(1):94–101, 1976. doi: https://doi.org/10.1016/0021-9797(76)90288-5.

[20] A. A. Lushnikov. Composition distributions of particles in a gelling mixture. *Physical Review E - Statistical, Nonlinear, and Soft Matter Physics*, 89(3):1–9, 2014. ISSN 15502376. doi:10.1103/PhysRevE.89.032121.

[21] A. A. Lushnikov. Exact kinetics of sol-gel transition in a coagulating mixture A. *Physical Review E - Statistical, Nonlinear, and Soft Matter Physics*, 73(3), 2006. ISSN 15393755. doi:10.1103/PhysRevE.73.036111.

[22] R. D. Vigil and R. M. Ziff. On the scaling theory of two-component aggregation. *Chemical Engineering Science*, 53(9):1725–1729, 1998. ISSN 00092509. doi: 10.1016/S0009-2509(98)00016-5.

[23] E. M. Hendriks, M. H. Ernst, and R. M. Ziff. Coagulation Equations with Gelation. *Journal of Statistical Physics*, 31(3):519–563, 1983. doi: https://doi.org/10.1007/BF01019497.

[24] H. Noureddini and D. C. Timm. Kinetic Analysis of Competing Intramolecular and Intermolecular Polymerization Reactions. *Macromolecules*, 25:1725–1730, 1992. doi:10.1021/ma00032a016.

[25] C. Sarmoria, E. M. Vallés, and D. R. Miller. Validity of Some Approximations Used To Model Intramolecular Reaction in Irreversible Polymerization Reference Model for Linear Polymerization. *Macromolecules*, 23:580–589, 1990. doi:10.1021/ma00204a034.

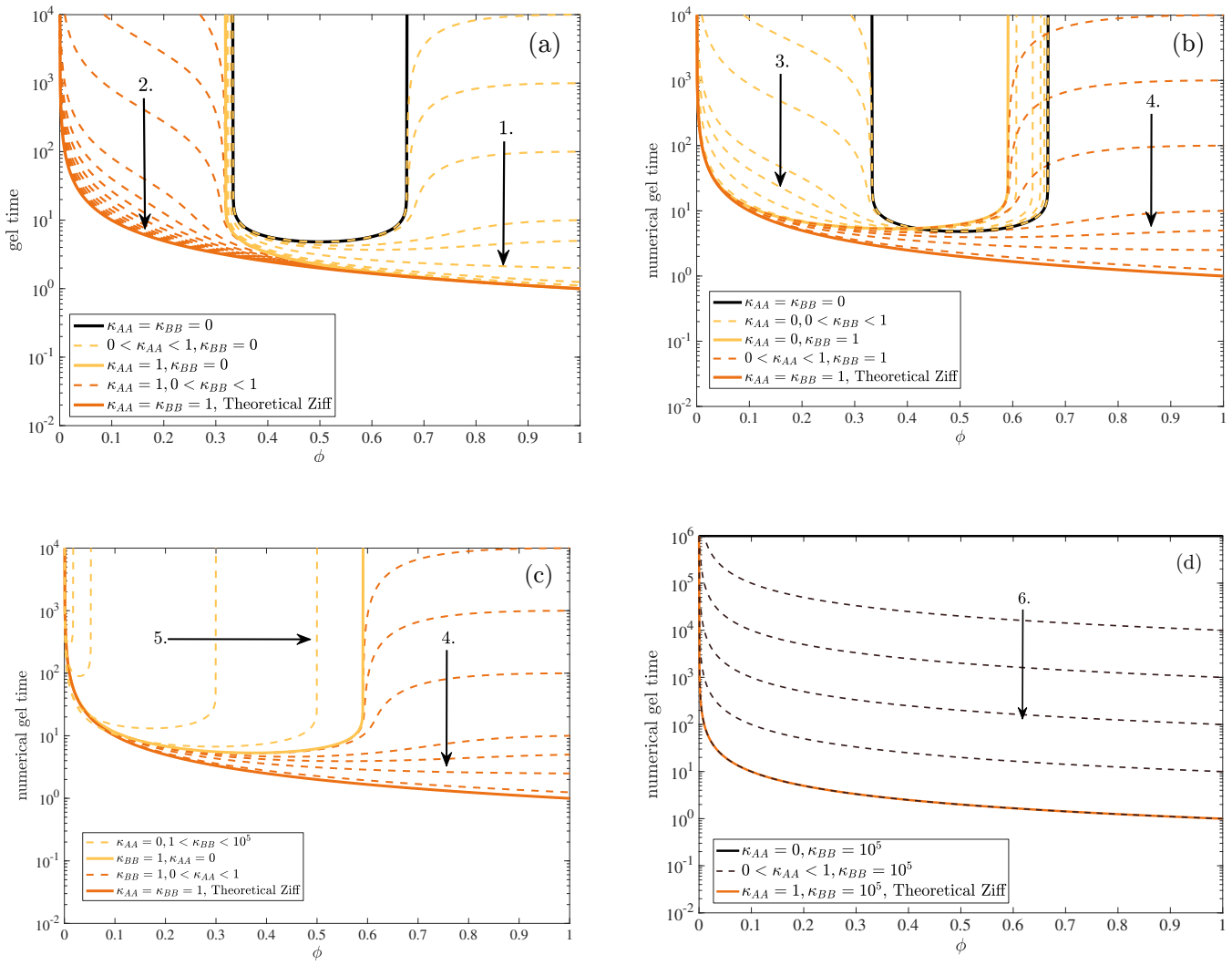

FIG. 12: Curves of numerical gel time as a function of ϕ for $f_A = 3$, $f_B = 2$ with dashed curves showing transitions as κ_{AA} and κ_{BB} vary along paths 1 – 6 in Figure 11.